Multiple configurations of the two excess 4*f* electrons on defective CeO_2(111): Origin and implications

Hui-Ying Li,[1] Hai-Feng Wang,[1] Xue-Qing Gong,[1] Yang-Long Guo,[1] Yun Guo,[1] Guanzhong Lu,[1] and P. Hu[2]
[1]*Labs for Advanced Materials, Research Institute of Industrial Catalysis, East China University of Science and Technology, 130 Meilong Road, Shanghai 200237, People's Republic of China*
[2]*School of Chemistry and Chemical Engineering, The Queen's University of Belfast, Belfast BT9 5AG, United Kingdom*
(Received 16 February 2009; published 6 May 2009)

Density-functional theory calculations have been carried out to systematically study single surface oxygen vacancies on CeO_2(111). It is surprisingly found that multiple structures with the two excess electrons localized at different positions can exist. We show that the origin of the multiconfigurations of 4*f* electrons is a result of geometric relaxation on the surface and strong localization characteristic of 4*f* electrons in ceria. The importance of 4*f* electron structures is also presented and discussed. These results may possess implications for our understanding of materials with *f* electrons.

DOI: 10.1103/PhysRevB.79.193401 PACS number(s): 61.72.jd, 82.65.+r, 68.35.Dv, 82.45.Jn

Oxygen vacancies on cerium dioxide (ceria, CeO_2) surfaces have attracted intense interest recently largely because of the following reasons: (i) CeO_2 and related materials find applications with extraordinary performance in many important catalytic processes such as crude oil refining, production of hydrogen, and control of vehicle emission[1–3] and (ii) their key role in these processes, e.g., storing and releasing oxygen as oxygen buffer, is mainly attributed to the surface O vacancies.[4] As the simplest case, the single oxygen vacancy has been investigated experimentally on different facets of ceria, especially the most often exposed (111) facet.[5–11] By performing high-resolution scanning tunneling microscopy (STM) and dynamic force microscopy (DFM) measurement of CeO_2(111), Esch *et al.*[7] and Torbrügge *et al.*[11] investigated O vacancy formation and the localization of *f* electrons was believed to be responsible for the observed O vacancy structures. It has been found that the removal of an O leads to an appearance of a newly formed occupied Ce 4*f* state in the gap between valence band and the previously empty Ce 4*f* states.[12]

Most work in the literature concentrated on the structure of single O vacancy and localization of the two 4*f* electrons in these materials. First-principles calculations have also been extensively used and some progresses have been made[7,13,14] in the field. In particular, 4*f* electrons were proposed to distribute at two Ce ions at the vacancies. Though many interesting experimental and theoretical results have been obtained, very few properties of CeO_2 closely related to its unique performance in applications were determined. Specifically, the following issues still remain to be tackled. (i) Although it is known that the two excess electrons in the presence of an O vacancy are localized in Ce 4*f* orbitals, it is not clear how they distribute in the system. This is a fundamental question due to the fact that many important properties in ceria, such as structures of O vacancies, O vacancy diffusion, and reactivity of ceria, are related to the electron distribution. In other words, in order to obtain insight into ceria and their applications, one must understand the electronic structure of the system. (ii) The question of what the physical origin is in such a distribution also remains to be answered. (iii) It is not clear either what the connection between the 4*f* electron distribution and surface reactivity of CeO_2 is. In the current work, we carried out a thorough investigation of the geometric and electronic structures of single O vacancy on CeO_2(111) using density-functional theory DFT+*U* calculations with a much bigger surface model compared to those in the literature to fully take into account relaxation effects, aiming at answering these questions.

The calculations have been performed within the generalized gradient approximation using the VASP code.[15] The project-augmented wave (PAW) method was used to represent the core-valence interaction, with [He] and [Xe] cores for oxygen and cerium, respectively. The valence electronic states were expanded in plane-wave basis sets with energy cutoff at 500 eV. The so-called DFT+*U* methodology has been extensively used[7,13,14] for ceria and it has been already showed that the approach can reproduce the experimental results, such as the STM images of reduced surface and relative positions of the vacancy-induced occupied gap state, with reasonable accuracy.[7] Therefore, in this study the DFT +*U* method was used to accurately reproduce the electronic and structural properties of CeO_2. The value of *U* was set to 5 eV as suggested in many other theoretic work.[14,16–18] The CeO_2(111) surface was modeled as a periodic slab with three CeO_2 atomic layers and the vacuum between slabs is $\sim$15 Å. A rather big $p(3\times4)$ surface cell with corresponding $1\times1\times1$ *k*-point mesh was used. The *k*-point sampling and the surface unit-cell size were checked. For example, using $p(4\times4)$ unit cell, in the most stable structures containing the top- and subsurface O vacancies, the O vacancy formation energies are 2.11 and 1.94 eV, respectively, which are 0.02 and 0.01 eV lower than those using $p(4\times3)$ surface unit cell, indicating that the interaction between defect states in neighboring supercells may be neglected. Accordingly, each surface cell contains 12 exposed Ce_{7c}, O_{3c}, and O_{4c}, respectively, and for single O vacancy, its coverage can be therefore estimated to be 1/12 ML. The adsorption was calculated on one side of the slab only and during structural optimization, all the atoms except those in the bottom CeO_2 atomic layer were allowed to move (force threshold is 0.02 eV/Å).

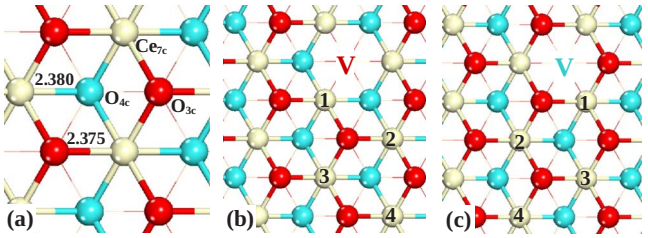

FIG. 1. (Color online) (a) Calculated structure of $CeO_2(111)$ (top view, bond length in Å) and illustrations of the $CeO_2(111)$ containing single (b) top-surface and (c) subsurface O vacancies. The exposed Ce_{7c} atoms are in white, O_{3c} in red (dark gray), and O_{4c} in blue (light gray). This notation is used throughout the paper. In (b) and (c), several exposed Ce atoms at the first-(1), second-(2), third-(3), and fourth-neighbor (4) positions with respect to the O vacancy (v) are labeled. Red V represents top-surface O vacancy and light-blue V subsurface O vacancy.

On $CeO_2(111)$, two types of lattice oxygen atoms are exposed, which are the threefold $O(O_{3c})$ on top surface and the fourfold one (O_{4c}) on subsurface [see Fig. 1(a)]. Accordingly, by removing them one can obtain the top-surface [Fig. 1(b)] and subsurface O vacancy [Fig. 1(c)], respectively. First, we calculated a single O vacancy formed by removing one top-surface O_{3c}. We found that there are indeed well-characterized Ce^{3+} ions on the surface, which can be seen from Fig. 2 in which the isosurface of excess spin charge density associated with the occupied gap state (about 1.2 eV above the valence-band edge) is incorporated with geometries. The two localized spin electrons have obvious f characteristics. In other words, one excess electron occupies a Ce $4f$ orbital and Ce^{4+} becomes Ce^{3+}, confirming the existence of $4f$ electron localization. However, it is surprising that there exist multiple configurations for $4f$ electrons to locate at various neighboring Ce ions. We found that the two excess electrons can actually localize at surface Ce ions at the first-, second-, third- and fourth-neighbor positions next to the vacancy [Fig. 1(b)] with similar energies. In Figs. 2(a)–2(g), we present the calculated structures corresponding to different f electron distribution patterns and the O vacancy formation energies estimated with respect to the gas phase O_2. It is interesting that the previously proposed structure with both the two Ce^{3+} at the first-neighbor positions [see Fig. 2(c)] was determined *not* to be energetically the most stable one. As shown in Fig. 2(a), the most stable structure contains the two Ce^{3+} both at the second-neighbor positions, giving rise to the O vacancy formation energy of 2.13 eV, which is ~0.2 eV lower than that of the first-neighbor structure (2.31 eV).

Second, we calculated the single surface O vacancy formed by removing one subsurface O_{4c}. Again, Ce^{3+} distributions in different configurations were determined. We show all the five structures incorporated with calculated spin charge densities in Figs. 2(h)–2(l), together with the calculated O vacancy formation energies. One can see that in the most stable structure, the two Ce^{3+} are again at the second-neighbor positions [Fig. 2(h)], similar to the case of top-surface vacancy. However, the calculated vacancy formation energy (1.95 eV) is ~0.2 eV lower than that of the top-surface vacancy [2.13 eV, Fig. 2(a)], suggesting that the subsurface vacancy is energetically more stable than the top-surface vacancy. Again, the previously proposed structure with both the two Ce^{3+} at first-neighbor positions [Fig. 2(k)]

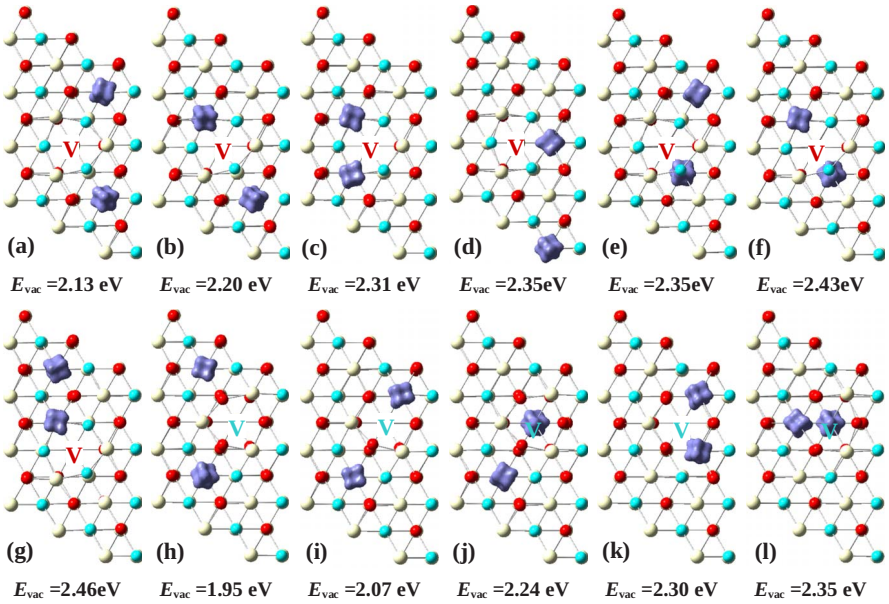

FIG. 2. (Color online) Calculated structures (top view) of the $CeO_2(111)$ surface containing single [(a)–(g)] top-surface and [(h)–(I)] subsurface O vacancy and the corresponding estimated vacancy formation energies (E_{vac}). The isosurface ($0.05e/Å^3$) of calculated spin charge densities are in dark blue. They are at two second-neighbor (a) Ce^{3+}, (b) first- and second-neighbor Ce^{3+}, (c) two first-neighbor Ce^{3+}, (d) first- and forth-neighbor Ce^{3+}, (e) first-neighbor Ce^{3+} in the second Ce layer and second-neighbor Ce^{3+}, (f) first-neighbor Ce^{3+} in the second Ce layer and first-neighbor Ce^{3+}, (g) first- and third-neighbor Ce^{3+}, with respect to the top-surface O vacancy; and (h) two second-neighbor Ce^{3+}, (i) separated first- and second-neighbor Ce^{3+}, first-neighbor Ce^{3+} in the second Ce layer and (j) second-neighbor Ce^{3+}, (k) two first-neighbor Ce^{3+}, (l) first-neighbor Ce^{3+} in the second Ce layer and first-neighbor Ce^{3+}, with respect to the subsurface O vacancy.

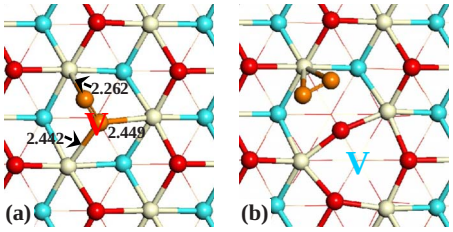

FIG. 3. (Color online) Calculated structures (top view) of single O_2 molecule adsorbed at the $CeO_2(111)$ containing single (a) top- and (b) subsurface O vacancy and the estimated adsorption energies (E_{ad}). The adsorbed O_2 is in orange.

was found to be considerably higher in vacancy formation energy (2.30 eV) compared to this structure. It should be mentioned that we also simulated STM images for our most stable structures. It is found that our calculated STM images agree well with experimental work.[7]

Is there any significance of these surprising results? To check this, we calculated the adsorption of O_2 molecules. This process was chosen since it is key to ceria's capacity as oxygen buffer and it is directly related to some catalytic reactions occurring on ceria.[19] Also, there exist many excellent experimental and theoretical studies for comparison.[20,21] On the $CeO_2(111)$ with a single top-surface O vacancy, the most favorable adsorption structure optimized from various starting geometries [Figs. 2(a)–2(g)] is shown in Fig. 3(a) and it gives the adsorption energy as high as 1.89 eV. One can see that in this structure, the O_2 molecule takes the site where the O_{3c} is missing and the two O atoms in the molecule bind with the three surface Ce ions at the first-neighbor positions. The O-O distance within the adsorbed O_2 (1.441 Å) is nearly the same as that reported by Huang and Fabris[21] for the peroxide (O_2^{2-}) species calculated on the $CeO_2(111)$ surface. Moreover, considering that the structure was determined to be spin unpolarized, it is likely that the adsorbed O_2 is an peroxide (O_2^{2-}) and the surface is reoxidized. It is worth mentioning that we also tested the adsorption of O_2 on an isolated Ce^{3+} with a top-surface vacancy and found that the triplet and singlet O_2 adsorption[22,23] energies are 0.04 and 0.01 eV, respectively, and both are very weak.

For O_2 adsorption on the $CeO_2(111)$ containing single subsurface O vacancy, very different results were obtained. O_2 molecule placed above the vacancy was found to be repelled by the protruding top-surface O_{3c} surrounding the subsurface vacancy and is unable to reach and fill the vacancy. On the other hand, the second-neighbor Ce^{3+} on the surface in the most stable configuration [Fig. 2(h)] was determined to be capable of taking one O_2 molecule. In Fig. 3(b), we illustrate the calculated structure of O_2 at this Ce^{3+} site, and the adsorption energy was estimated to be 0.37 eV. As one can see, both the two O atoms in the O_2 molecule bind with the same Ce. The O-O bond of the adsorbed O_2 was found to be 1.335 Å. This bond length is very close to that of very reactive superoxide (O_2^-) species proposed in early work.[21] Moreover, the electronic analysis of this system [Fig. 3(b)] also shows that the adsorbed O_2 contains one excess electron transferred from the surface Ce it attaches to. Therefore, we believe that O_2 sitting around the subsurface O vacancies of the $CeO_2(111)$ becomes superoxide O_2^-.

In the above, we have presented the results of our systematic calculations of defective $CeO_2(111)$ containing single O vacancy at top- and subsurface and their reactivities toward adsorption of O_2 molecule. Most significantly, multiple Ce^{3+} distributions were determined, and the separation of the two Ce^{3+} at the second-neighbor positions of the vacancy gives the most stable structure and induces the formation of highly reactive superoxide O_2^-,[19,21] which has been widely detected experimentally in catalytic reactions. The above results thus may be of importance in understanding the unique property of ceria in three-way catalysts. Then an interesting question is what is the physical origin of finding the existence of multiple configurations of f electrons in the presence of an O vacancy? We believe that such capacity of ceria can be mainly attributed to the following two factors. (i) The geometric factor: first, the coordination number of Ce in ceria is 8 compared, for example, to Al in Al_2O_3 being 6, and consequently there exist many different ways for the O atoms to relax to compensate for the missing Ce-O bonds. Second, ceria possesses a fluorite structure which is quite open. Therefore, there are multiple relaxed structures with similar energies in the presence of an O vacancy, each being a local minimum structure. (ii) Localization of $4f$ electrons: $4f$ electrons are highly localized and do not involve in bonding in ceria. Once an O atom is removed from $CeO_2(111)$, the two excess electrons should be accepted by f orbitals in two Ce ions. Which Ce $4f$ orbital should be occupied by the excess electrons depend on the geometric structure. We carefully examined all the geometric structures with top-surface and subsurface O vacancies and found that the $4f$ electron is always in the Ce ion with longest average Ce-O distance. This result can be understood as follows. Due to the localization of $4f$ electrons, the two excess electrons will always be in two separated Ce ions and the competition for the excess electrons among all the Ce ions near an O vacancy will naturally result in the Ce ions with the weakest Ce-O bonding being favored. To illustrate this point, here we describe the most stable geometric structure in the presence of top-surface O vacancy, in which the two f electrons are well separated [Fig. 2(a)]. We can see that the two O atoms next to the O vacancy undergo deep relaxation. The bond lengths between the two O atoms and the second-neighbor Ce ion, to which the O atoms bind, increase from the average bond length of ~2.38 Å in bulk ceria to 2.592 and 2.610 Å, respectively. In fact, the relaxation is so deep that the two second-neighbor Ce ions lose contact with the relaxed surface O, resulting in the localization sites for the excess electrons.

Structural relaxation not only determines the distribution of localized electrons, it is also directly related to the relative stabilities of surfaces containing top- and subsurface O vacancies and their reactivities. On the defective surface with single top-surface vacancy, the three nearest O atoms around the vacancy are all subsurface bulklike O_{4c} that are binding with four Ce ions. In contrast, the nearest three O around a subsurface O vacancy are all threefold, which can be expected to be more mobile compared to the fourfold ones. Therefore, deeper relaxation would occur on the surface with

single subsurface O vacancy compared to that with top-surface vacancy and gives rise to a lower vacancy formation energy (1.95 vs 2.13 eV). For O_2 adsorption at one isolated second-neighbor Ce^{3+} [Figs. 2(a) and 2(h)], the interaction between O_2 and Ce^{3+} also requires significant structural relaxation of the surface O between the Ce^{3+} and the vacancy. This occurs easily at the subsurface vacancy [Fig. 3(b), E_{ad} =0.37 eV] and O_2^- is subsequently generated but again is infeasible at the top-surface one which only takes O_2 at the vacancy. From the above discussions, we can learn that defects with different geometric and corresponding electronic structures on $CeO_2(111)$ can exhibit storing or promoting capacity toward O_2. In particular, we can expect that subsurface O vacancies surrounded by very mobile threefold O atoms and capable of generating active oxygen species without being filled would play an active role in the structures and reactivities of defective $CeO_2(111)$ (Refs. 7 and 11).

The localization of 4*f* electrons in ceria has been reported in the literature. The current work reveals clearly some interesting consequences of the *f* electron localization. Together with the quite open geometric structure, ceria exhibits some unique properties for distributions of localized *f* electrons in structural relaxation induced by, for example, the occurrence of lattice oxygen vacancies. Furthermore, the way for these electrons to distribute is exclusively determined by local bonding configurations and closely related to the material's performance in interacting with active species such as O_2. Because O vacancies are common defects in oxides, the findings in this work may have some significant implications for understanding other oxides.

In summary, we report that the two excess electrons in the presence of an O vacancy are in fact separated in multiple ways on $CeO_2(111)$, which may be a fundamental characteristics of materials with *f* electrons. The physical origin of the finding is mainly attributed to the surface relaxation and *f* electron localization and the evidence of a structure generating active O_2^- is presented. We expect that these results can help us to understand many properties of ceria. They may also have significant implications in many applications of ceria and other related materials.

Note added. Recently, it has come to our attention that results similar to ours were obtained independently by Ganduglia-Pirovano *et al.*[24]

This work is financially supported by the National Basic Research Program (Grant No. 2004CB719500), the International Science and Technology Cooperation Program (Grant No. 2006DFA42740), the 111 Project (Grant No. B08021), and the National Natural Science Foundation of China (Grants No. 20703017 and No. 20601008). X.Q.G also thanks ECUST for the startup funding (Grant No. YJ0142142).

[1] G. A. Deluga, J. R. Salge, L. D. Schmidt, and X. E. Verykios, Science **303**, 993 (2004).
[2] K. Otsuka, T. Ushiyama, and I. Yamanaka, Chem. Lett. **22**, 1517 (1993).
[3] S. Park, J. M. Vohs, and R. J. Gorte, Nature (London) **404**, 265 (2000).
[4] A. Trovarelli, *Catalysis by Ceria and Related Materials* (Imperial College, UK, 2002).
[5] H. Nörenberg and G. A. D. Briggs, Phys. Rev. Lett. **79**, 4222 (1997).
[6] H. Nörenberg and G. A. D. Briggs, Surf. Sci. **424**, L352 (1999).
[7] F. Esch, S. Fabris, L. Zhou, T. Montini, C. Africh, P. Fornasiero, G. Comelli, and R. Rosei, Science **309**, 752 (2005).
[8] K. Fukui, Y. Namai, and Y. Iwasawa, Appl. Surf. Sci. **188**, 252 (2002).
[9] Y. Namai, K. Fukui, and Y. Iwasawa, Catal. Today **85**, 79 (2003).
[10] Y. Namai, K. Fukui, and Y. Iwasawa, J. Phys. Chem. B **107**, 11666 (2003).
[11] S. Torbrügge, M. Reichling, A. Ishiyama, S. Morita, and O. Custance, Phys. Rev. Lett. **99**, 056101 (2007).
[12] D. R. Mullins and S. H. Overbury, Surf. Sci. **511**, L293 (2002).
[13] S. Fabris, G. Vicario, G. Balducci, S. de Gironcoli, and S. Baroni, J. Phys. Chem. B **109**, 22860 (2005).
[14] M. Nolan, S. C. Parker, and G. W. Watson, Surf. Sci. **595**, 223 (2005).
[15] G. Kresse and J. Hafner, Phys. Rev. B **49**, 14251 (1994); G. Kresse and J. Furthmüller, Comput. Mater. Sci. **6**, 15 (1996).
[16] M. Nolan, S. Grigoleit, D. C. Sayle, S. C. Parker, and G. W. Watson, Surf. Sci. **576**, 217 (2005).
[17] M. Nolan, S. C. Parker, and G. W. Watson, J. Phys. Chem. B **110**, 2256 (2006).
[18] M. Nolan and G. W. Watson, J. Phys. Chem. B **110**, 16600 (2006).
[19] V. V. Pushkarev, V. I. Kovalchuk, and J. L. d'Itri, J. Phys. Chem. B **108**, 5341 (2004).
[20] Y. M. Choi, H. Abernathy, H.-T. Chen, M. C. Lin, and M. Liu, ChemPhysChem **7**, 1957 (2006).
[21] M. Huang and S. Fabris, Phys. Rev. B **75**, 081404(R) (2007).
[22] W. Orellana, A. J. R. da Silva, and A. Fazzio, Phys. Rev. Lett. **90**, 016103 (2003).
[23] K. Kato, T. Uda, and K. Terakura, Phys. Rev. Lett. **80**, 2000 (1998).
[24] M. V. Ganduglia-Pirovano, J. L. F. Da Silva, and J. Sauer, Phys. Rev. Lett. **102**, 026101 (2009).